Nanoparticle Stability

International Edition: DOI: 10.1002/anie.201705422
German Edition: DOI: 10.1002/ange.201705422

Assessing the Stability of Fluorescently Encoded Nanoparticles in Lysosomes by Using Complementary Methods

*Ana M. Milosevic, Laura Rodriguez-Lorenzo, Sandor Balog, Christophe A. Monnier, Alke Petri-Fink, and Barbara Rothen-Rutishauser**

Abstract: *Nanoparticles (NPs) are promising tools in biomedical research. In vitro testing is still the first method for initial evaluation; however, NP colloidal behavior and integrity, in particular inside cells (that is, in lysosomes), are largely unknown and difficult to evaluate because of the complexity of the environment. Furthermore, while the majority of NPs are usually labeled with fluorescent dyes for tracking purposes, the effect of the lysosomal environment on the fluorophore properties, as well as the ensuing effects on data interpretation, is often only sparsely addressed. In this work, we have employed several complementary analytical methods to better understand the fate of fluorescently encoded NPs and identify potential pitfalls that may arise from focusing primary analysis on a single attribute, for example, fluorophore detection. Our study shows that in a lysosomal environment NPs can undergo significant changes resulting in dye quenching and distorted fluorescence signals.*

Engineered nanoparticles (NPs) are opening exciting new avenues for both diagnostic and therapeutic opportunities in treating diseases.[1] Therefore, it is imperative that researchers develop and employ adequate methodologies to study the relationships between NPs, their physico-chemical properties, uptake at the cellular level, and possible cell response.[2–4] Herein, we propose that NP performance should be investigated beyond initial uptake, that is, with a special emphasis on the fate of the NPs once they reach the lysosomes. More importantly, the fate of their integral components, on which we rely for detection (fluorescence being the most common one), should not be neglected. While many different methods are used to characterize NPs and their association with single cells, as well as their cellular uptake (that is, fluorescence activated cell sorting (FACS), inductively coupled plasma (ICP) spectroscopy, and imaging techniques such as fluorescence microscopy), it is not clear whether the different techniques provide the same information.[5–8] Therefore, it is not only crucial to establish standard analytical techniques along with reliable and validated controls to study intracellular fate of NPs but also essential to promote the use of complementary methods that account for different NP properties.

The aim of this work was thus to investigate the influence of the intracellular environment, specifically the lysosomal environment, on the physicochemical properties of fluorescence-encoded gold NPs (AuNPs). This was done by employing different analytical methods that address and quantify different NP properties. We used mouse macrophage J774 A.1 cells as a model for professional phagocytic cells, since they usually exhibit significant NP uptake through various endocytic pathways, as shown previously for other particle types.[9] Fluorescence-encoded AuNPs (COOH PVA ATTO590 AuNPs) were comprised of two layers of ATTO590-conjugated poly(vinyl alcohol) (PVA) and unlabeled PVA surrounding AuNPs (Figure 1). In doing so, the ATTO590 dye was shielded by the second (PVA) layer. It has been previously reported that surface-exposed dye molecules, such as non-shielded ATTO590, interfere with cellular

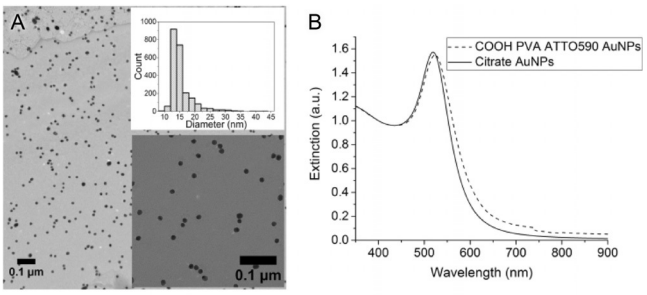

C

NP type	Size TEM d_c (nm)	DDLS d_h (nm)	Zeta-potential (mV)	Dye/NP
Citrate AuNPs	16.5 ± 3.7	28 ± 1	- 44.25 ± 1.2	n.a.[1]
COOH PVA ATTO590 AuNPs	16.5 ± 3.7	43 ± 2	-5.82 ± 0.91	120

[1] Not applicable. Citrate AuNPs were not functionalized with fluorescent dye.

Figure 1. Characterization of functionalized AuNPs. A) TEM images of AuNPs at two magnifications and the size distribution histogram. B) UV/Vis spectrum of citrate and COOH PVA ATTO590 functionalized AuNPs. Spectra are normalized to 400 nm. C) Table summarizing size, zeta potential, and labeling efficiency. Size measurements, where d_c is diameter of the core and d_h the hydrodynamic diameter, were obtained by TEM and DDLS, respectively.

[*] A. M. Milosevic, Dr. L. Rodriguez-Lorenzo, Dr. S. Balog, Dr. C. A. Monnier, Prof. Dr. A. Petri-Fink, Prof. Dr. B. Rothen-Rutishauser
Adolphe Merkle Institute, University of Fribourg
Ch. des Verdiers 4, Fribourg, 1700 (Switzerland)
E-mail: barbara.rothen@unifr.ch

Supporting information, including experimental details, and the ORCID identification number(s) for the author(s) of this article can be found under: https://doi.org/10.1002/anie.201705422.

uptake. This makes shielded NPs favorable candidates, since the polymer used provides protection from the dye while the fluorescence remains uncompromised.[7] AuNPs were selected as model NPs not only for their well-established synthetic procedure but also because they did not show any adverse effects in previous in vitro[10] or in vivo[11] studies. Moreover, the fluorescent dye allows the detection and quantification by flow cytometry, fluorescence spectroscopy, and imaging techniques, hence allowing the direct tracking of the fate of NPs. Figure 1 summarizes the full characterization of these NPs, which had a core diameter of 16.5 nm, a hydrodynamic diameter of 42 nm, and a negative zeta potential of −5.8 mV (see Table in the Figure 1). The AuNPs remained colloidally stable in complete cell culture media, and no significant changes in the hydrodynamic size were observed over 24 h of incubation at 37 °C (Supporting Information, Figure S1). Fluorescence measurements of functionalized NPs in PBS showed that the synthesized NPs provided a strong fluorescence signal. Incubation in complete cell culture media also did not affect the fluorescence properties (Supporting Information, Figures S2–S4).

After 24 h of exposure at 37 °C to J774 A.1 cells, NP-associated fluorescent signal was not detected by confocal laser scanning microscopy (LSM) within the intracellular space, as shown in Figure 2 A. However, dark spots were visible within the cells in bright-field optical microscopy images, indicating an uptake of the NPs (Figure 2, white arrow in the BF image inset). To confirm this assumption, we used dark-field hyperspectral optical microscopy (DF-HSI (Cytoviva®)), which enables a fluorescence-independent visualization generated by light scattered from plasmonic NPs.[12,13] By using this method, AuNPs were clearly visualized within the cells, appearing as bright spots (see representative image in Figure 2).

NP uptake was further investigated by FACS (Figure 2) and ICP-OES. Figure 2 shows that flow cytometry also evinced only low signals, which could be interpreted as low NP uptake; whereas ICP-OES, a sensitive elemental analysis technique, which allows the quantification of elemental gold,[6] showed that approximately 2×10^5 AuNPs per cell (5.91 pg per cell), that is, more than 60 % of the total number (mass) of NPs used for the exposure experiment, were either internalized or cell-associated after 24 h. Short incubation times (5 min, 30 min, and 4 h) did not provide any additional information on NPs at early stages of cellular uptake,[14] since NP uptake was too low to provide solid information on NP fluorescence and stability based on LSM, DF-HIS, and ICP-OES (Supporting Information, Figure S5).

In all, these findings highlight the circumstantial shortcomings of traditionally employed fluorescence-based analytical techniques for fluorescent NPs in vitro as well as in vivo. Although LSM or FACS are often used to study cellular uptake, fluorophore leakage, bleaching, or quenching of the dye might strongly influence the results, subsequently leading to inaccurate interpretation of the data. In addition, it has been previously shown that the attachment of fluorescent dyes to the NP surface can conceal fundamental particle properties and modulate cellular uptake.[7] Hence, in order to obtain unbiased results, fluorescence-based data should always be correlated with other analytical methods such as dark-field microscopy or ICP-based spectroscopy techniques.

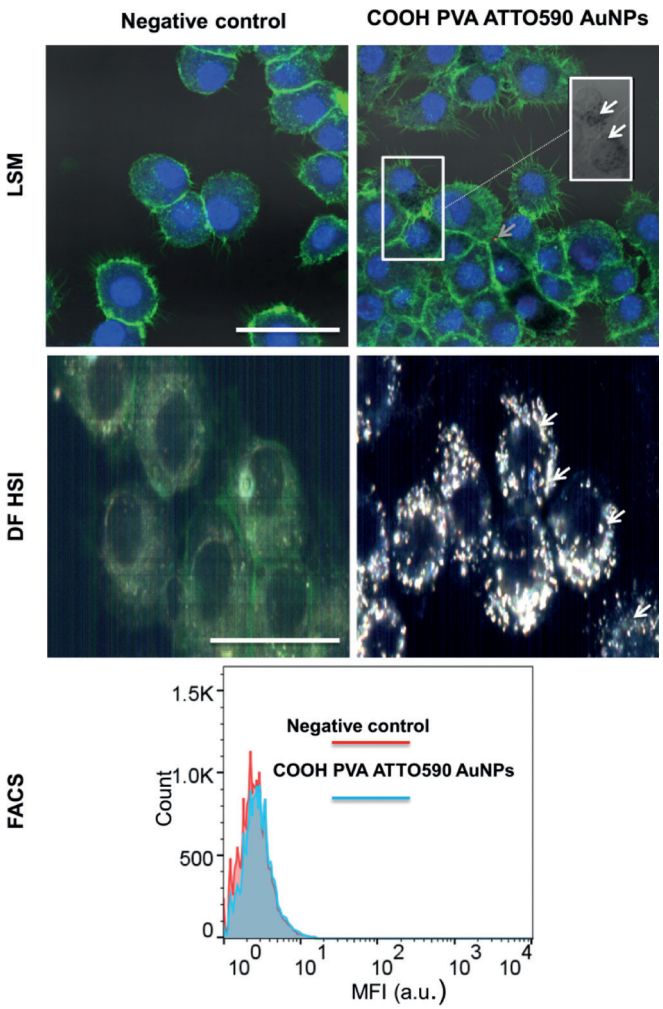

Figure 2. J774.A.1 mouse macrophages were exposed to 20 μg mL^{-1} of COOH PVA ATTO590 AuNPs for 24 h and fluorescence was detected by LSM and flow cytometry. LSM: Cells were stained with the nucleus stain DAPI (blue), F-actin stain phalloidin Alexa 488 (green), and particles are labeled with the ATTO590 dye (red). White arrows point to NPs, as well as the aggregates for COOH PVA AuNPs, which can be observed in the BF (bright-field) window (inset). Fluorescent signal is detected only for non-internalized NPs (grey arrow) as opposed to NPs located in the cells. Scale bar = 20 μm. DF HSI: Dark field hyperspectral imaging microscopy of NPs inside J774.A.1 mouse macrophages. The image was formed based on spectral information of each pixel, where, due to the intensity of light scattering, AuNPs give the brightest signal. FACS: Flow cytometry data for COOH PVA AuNPs exposed cells does not exhibit a significant increase in fluorescence when compared to the negative control.

In a next step, we systematically investigated the impact of the lysosomal environment on the physicochemical properties of the NPs, with a particular emphasis on their fluorescence properties, given their importance in not only detecting and quantifying NPs but also for evaluating their colloidal stability within a cell as well. Some previous in vivo and in vitro studies have shown that the integrity of NPs can be compromised. In fact, the protein corona surrounding NPs begins to disintegrate at short incubation times, that is, 8 h.[15–17] Despite these

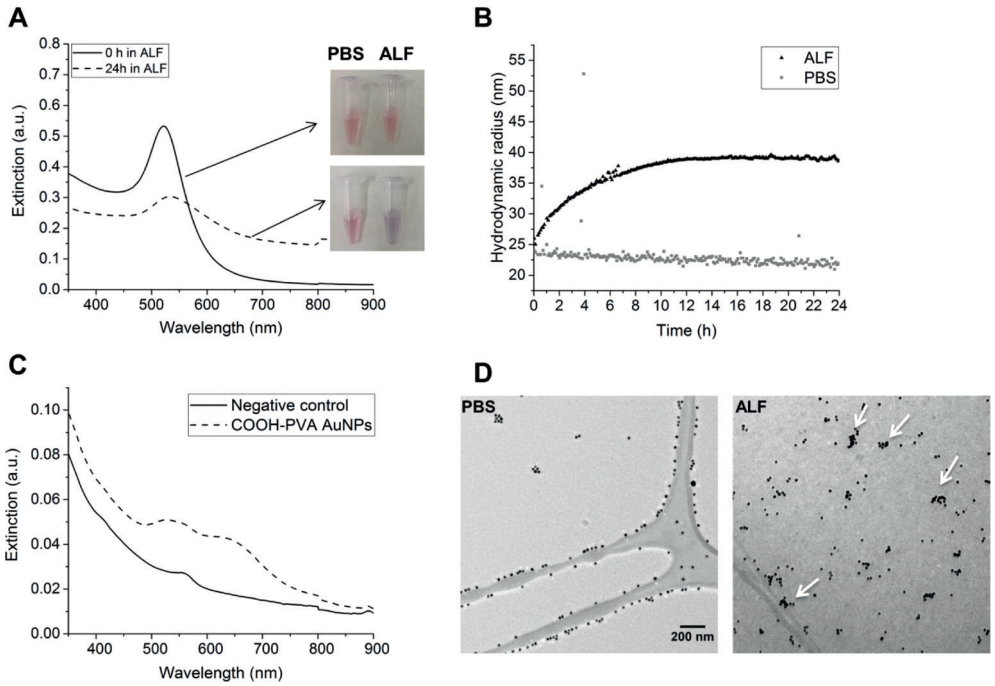

Figure 3. Observation of size increase and destabilization of NPs. A) UV/Vis spectra were measured at the beginning and after 24 h of incubation at 37 °C in ALF showing a band broadening and red shift (size increase) for COOH PVA AuNPs incubated in ALF for 24 h. Inset images show the NP solution at the beginning and after 24 h incubation in both PBS and ALF revealing a color shift for the particles after 24 h in ALF. B) DDLS measurements were performed over 24 h at 37 °C in both ALF and PBS also indicating an aggregation in ALF over time. C) J774 cells were exposed to 20 μg mL^{-1} of COOH PVA-functionalized NPs over 24 h and lysosomes containing the AuNPs were isolated. UV/Vis spectra show two signal bands characteristic for the AuNP aggregates. D) Observation of the NPs aggregation by CryoEM. Particles were first incubated for 24 h at 37 °C in both PBS and ALF, which was followed by sample preparation. Imaging under native conditions (particle stability was not affected by the drying effect) shows that stability of NPs (both particle types) was not affected by the incubation in PBS, whereas COOH PVA AuNPs show signs of aggregation after incubation in ALF. White arrows point to COOH PVA AuNP aggregates.

reports, we focused on a 24 h exposure time, as we only observed minimal cellular uptake at earlier time points (Figure S5). Given that endocytosis is the general NP entry mechanism, NPs initially end up in early and late endosomes that subsequently fuse with lysosomes,[3,4,18] which are complex digestive organelles that have a low pH (ca. 4.5) and a salt-rich environment filled with hydrolytic enzymes,[19] we explored the stability of the NPs in artificial lysosomal fluid (ALF) by UV/Vis spectroscopy and depolarized dynamic light scattering (DDLS) over 24 h at 37 °C. ALF has a well-known chemical composition and imitates the complex environment of lysosomes (with the exception of proteolytic enzymes).[20] The AuNPs were incubated in ALF as well as in PBS as a control. Prior to incubation in ALF, NPs were transferred from PBS to MiliQ water, since sodium chloride and phosphate ions could interfere with the ALF components. This transfer did not affect the NPs' colloidal stability, as confirmed by DDLS (Supporting Information, Figure S6). UV/Vis spectra (Figure 3A) in ALF, but not in PBS, show a red shift, significant band broadening, and increased absorbance in the near infrared region (NIR) after 24 h of incubation, which is characteristic for AuNPs aggregates, as previously described.[21] Furthermore, DDLS revealed an increase in hydrodynamic size of approximately 20 nm (Figure 3B) and a sudden decrease in scattering intensity after an initial steady increase, which could be explained by NP sedimentation resulting from aggregation or increase in shell density (Supporting Information, Figure S7). In our case, the surface grafted polymer is attached to the NPs through electrostatic interaction enabling conformational changes of the polymer in solution[22–24] and possibly acts to stabilize some of the early stages of aggregation, while the larger aggregates are not clearly detectable with DDLS because of the above-mentioned sedimentation.

In order to understand why particles aggregate in ALF, we repeated the experiments using phosphate buffer (pH 4.5), which corresponds to the acidic pH of ALF. DDLS did not reveal any change in the hydrodynamic size of the NPs (Supporting Information, Figure S8), indicating that the high ionic strength and the presence of other organic molecules (for example, glycine, sodium tartrate, sodium lactate, and sodium pyruvate) in ALF also play important roles in the decrease of colloidal stability.

We then reverted to cryo-transmission electron microscopy (CryoTEM) to visualize the aggregation of the AuNPs while avoiding common drying artefacts.[25] These investigated NPs, incubated in PBS (as a negative control) or ALF for 24 h at 37 °C, were preserved in a thin layer of vitreous ice for analysis. As shown in Figure 3C, the AuNPs were very well dispersed in PBS, whereas there were clear signs of aggregation when they were incubated in ALF (white arrow in Figure 3D). Aggregates of different sizes, as well as a low percentage of single NPs were observed, supporting the DDLS data, in which the overall average increase in size was around 20 nm. These findings were also well in line with the UV/Vis spectroscopy data, in which not only a red shift but also a significant band broadening was observed, thus indicating the presence of aggregates of varying sizes, which contribute to the absorption in different parts of the spectra.

Following this, we analyzed the intracellular occurrence of the AuNPs directly in crude lysosomal fractions to further elucidate the effect of the lysosomal environment, in which, in addition to high salt concentration and low pH, both enzymes and a confined space contribute to an even more specific

environment.[19] Lysosomes were thus isolated after exposing J774.1 cells to NPs for 24 h (described in the Supporting Information), followed by UV/Vis spectroscopy and DDLS analysis. The occurrence of two bands in the UV/Vis spectra and clear absorbance in the NIR spectra (Figure 3D) show that aggregation was even more prominent in isolated lysosomes than in ALF (Figure 3A). The presence of AuNP aggregates in the crude lysosomes was also confirmed by DDLS measurements, which showed a strong increase in hydrodynamic size to around 358 nm. These findings confirm that the spatial confinement and the presence of high molecular weight molecules, for example, enzymes, are also relevant in the NP destabilization process inside lysosomes.

We then examined the effects of ALF on the ATTO590 fluorescence properties alone in an effort to investigate the relationship between the fluorescence decay and the colloidal destabilization. Although a significant decrease of fluorescence was observed in ALF, a complete quenching (as observed in the cell studies) did not occur (Figures S2 and S3). Hence, any further fluorescence loss of the fluorophore in the polymer sandwich may be attributed to desorption of the dye functionalized polymer and/or quenching of the dye owing to close proximity to the gold surface. To study possible polymer desorption, the functionalized NPs were incubated in both PBS and ALF for 24 h at 37 °C. Following the incubation and centrifugation, the amount of polymer in the supernatant was measured based on a colorimetric assay, in which PVA forms a characteristic blue complex with a KI/I_2/boric acid mixture.[26] Based on the obtained data, we could not attribute the previously observed aggregation and fluorescence decay to polymer desorption, since a substantial polymer loss could not be observed in either PBS or ALF (Supporting Information, Table S1). However, because of the limitations of colorimetric techniques it cannot be excluded that a fraction of the polymer is degraded, which ultimately contributes to the overall effect, as previously reported by Kreyling et al.[16]

In a final step, the possibility of a change in the Au surface–dye distance as a consequence of a COOH-PVA conformational change was explored. The polymer was incubated in PBS or ALF at 37 °C and the hydrodynamic size changes were measured by conventional DLS (experimental procedure in the Supporting Information). In PBS, the polymer showed uniform and reproducible values of around 14 nm in diameter. The polymer solution became turbid once the polymer was incubated in ALF. This was clearly due to the increase of the hydrodynamic size (up to 450 nm in diameter), indicating that the conformation and size of the polymer has changed (Supporting Information, Figure S9). The effect of this conformational change on the fluorescence decay was then further investigated using surface enhanced Raman scattering (SERS; Figure 4).

Upon excitation with a laser (633 nm), the intensity of the SERS signal from ATTO590 changes, depending on the distance to the metal NP.[27] If the molecule is in close proximity to the metal, fluorescence will be quenched, whereas if the molecule is close but not attached to the metal NP, it will be affected by the electromagnetic field enhancement generated by the AuNPs and the Raman signal increases. When AuNPs were incubated in PBS and excited with the 633 nm laser, the recorded SERS intensity was very weak. However, the intensity notably increased, approximately 6-fold, when AuNPs were incubated in ALF. From these results, we concluded that when the AuNPs are incubated/internalized in ALF/lysosomes, the polymer layer swells causing AuNPs aggregation, while leaving the ATTO590 molecules trapped closer to the Au cores, as indicated by notable increases of SERS signals, thus explaining the fluorescence quenching.

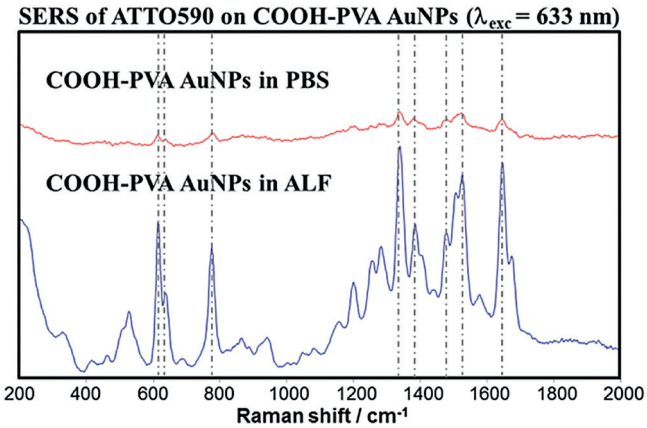

Figure 4. Surface-enhanced Raman scattering (SERS) spectra (λ_{exc} = 633 nm) of ATTO590 on functionalized AuNPs in both PBS and ALF after 24 h incubation. The enhancement of the Raman intensity (6.5×) in ALF indicates that the fluorescent dye–gold surface distance decreased, demonstrating that the loss of fluorescence is due to dye quenching by the gold surface.

In summary, we have shown that the lysosomal environment, that is, an acidic and confined space, can have an impact on polymer-grafted NPs with incorporated fluorophores. The stability and integrity of negatively charged and fluorescently labeled PVA AuNPs were strongly affected by a high salt content and low pH environment, such as that within lysosomes, not only causing the aggregation of NPs but also resulting in a loss of fluorescence, which in this case, leads to data misinterpretation.

It should be noted that potential NP disintegration, depending on the NP type and time frame, can have similar consequences.[15] Based on our data, a combination of different analytical techniques based on different NP properties (for example, scattering vs. fluorescence) is advised to investigate the lysosomal stability of NPs and to confirm the stability of a fluorescent dye using ALF and crude lysosomal fractions in view of redesigning efficient and safe NP formulations. On the other hand, a fluorescent dye incorporated into the structure of NPs, like in the case of fluorescent silica NPs,[28] would require another approach since the dye is more protected from the influence of the environment.

Acknowledgements

This study was supported by the National Center of Competence in Research (NCCR) for Bio-Inspired Materials and the Adolphe Merkle Foundation. We thank our former

summer student William Gaffney from Durham University for his assistance on the project during the summer 2016 and Miguel Spuch for the TOC Figure. The Dr. Alfred Bretscher fund is gratefully acknowledged, and access to the electron microscopy was provided by the Microscopy Imaging Center (University of Bern).

Conflict of interest

The authors declare no conflict of interest.

Keywords: fluorescence · lysosomes · nanoparticles · stability · uptake detection

How to cite: *Angew. Chem. Int. Ed.* **2017**, *56*, 13382 – 13386
Angew. Chem. **2017**, *129*, 13567 – 13571

[1] J. Shi, A. R. Votruba, O. C. Farokhzad, R. Langer, *Nano Lett.* **2010**, *10*, 3223 – 3230.
[2] M. C. M. Daniel, D. Astruc, *Chem. Rev.* **2004**, *104*, 293 – 346.
[3] C. Mühlfeld, B. Rothen-Rutishauser, F. Blank, D. Vanhecke, M. Ochs, P. Gehr, *Am. J. Physiol. Lung Cell. Mol. Physiol.* **2008**, *294*, L817 – L829.
[4] K. Unfried, C. Albrecht, L. Klotz, A. Von Mikecz, S. Grether-Beck, R. P. F. F. Schins, A. Von, S. Grether-Beck, R. P. F. F. Schins, *Nanotoxicology* **2007**, *1*, 52 – 71.
[5] B. Drasler, D. Vanhecke, L. Rodriguez-Lorenzo, A. Petri-Fink, B. Rothen-Rutishauser, *Nanomedicine* **2017**, nnm-2017-0071.
[6] D. Vanhecke, L. Rodriguez-Lorenzo, M. J. D. Clift, F. Blank, A. Petri-Fink, B. Rothen-Rutishauser, *Nanomedicine* **2014**, *9*, 1885 – 1900.
[7] L. Rodriguez-Lorenzo, K. Fytianos, F. Blank, C. Von Garnier, B. Rothen-Rutishauser, A. Petri-Fink, *Small* **2014**, *10*, 1341 – 1350.
[8] C. Gottstein, G. Wu, B. J. Wong, J. A. Zasadzinski, *ACS Nano* **2013**, *7*, 4933 – 4945.
[9] D. A. Kuhn, D. Vanhecke, B. Michen, F. Blank, P. Gehr, A. Petri-Fink, B. Rothen-Rutishauser, *Beilstein J. Nanotechnol.* **2014**, 1625 – 1636.
[10] K. Fytianos, S. Chortarea, L. Rodriguez-Lorenzo, F. Blank, C. Von Garnier, A. Petri-Fink, B. Rothen-Rutishauser, *ACS Nano* **2017**, *11*, 375 – 383.
[11] E. Seydoux, L. Rodriguez-Lorenzo, R. A. M. Blom, P. A. Stumbles, A. Petri-Fink, B. M. Rothen-Rutishauser, F. Blank, C. von Garnier, *Nanomed. Nanotechnol. Biol. Med.* **2016**, *12*, 1815 – 1826.
[12] A. L. Chen, Y. S. Hu, M. a. Jackson, A. Y. Lin, J. K. Young, R. J. Langsner, R. a. Drezek, *Nanoscale Res. Lett.* **2014**, *9*, 454.
[13] G. A. Roth, S. Tahiliani, N. M. Neu-Baker, S. A. Brenner, *Wiley Interdiscip. Rev. Nanomed. Nanobiotechnol.* **2015**, *7*, 565 – 579.
[14] G. Levkowitz, H. Waterman, E. Zamir, Z. Kam, S. Oved, W. Y. Langdon, L. Beguinot, B. Geiger, Y. Yarden, *Genes Dev.* **1998**, *12*, 3663 – 3674.
[15] N. Feliu, D. Docter, M. Heine, P. Del Pino, S. Ashraf, J. Kolosnjaj-Tabi, P. Macchiarini, P. Nielsen, D. Alloyeau, F. Gazeau, et al., *Chem. Soc. Rev.* **2016**, *45*, 2440 – 2457.
[16] W. G. Kreyling, A. M. Abdelmonem, Z. Ali, F. Alves, M. Geiser, N. Haberl, R. Hartmann, S. Hirn, D. J. de Aberasturi, K. Kantner, et al., *Nat. Nanotechnol.* **2015**, *10*, 619 – 623.
[17] F. Bertoli, D. Garry, M. P. Monopoli, A. Salvati, K. A. Dawson, *ACS Nano* **2016**, *10*, 10471 – 10479.
[18] S. Zhang, H. Gao, G. Bao, *ACS Nano* **2015**, *9*, 8655 – 8671.
[19] H. Appelqvist, P. Wäster, K. Kågedal, K. Öllinger, *J. Mol. Cell Biol.* **2013**, *5*, 214 – 226.
[20] W. Stopford, J. Turner, D. Cappellini, T. Brock, *J. Environ. Monit.* **2003**, *5*, 675 – 680.
[21] V. Hirsch, C. Kinnear, L. Rodriguez-Lorenzo, C. A. Monnier, B. Rothen-Rutishauser, S. Balog, A. Petri-Fink, *Nanoscale* **2014**, *6*, 7325 – 7331.
[22] X.-Z. Cao, H. Merlitz, C.-X. Wu, G. Ungar, J.-U. Sommer, *Nanoscale* **2016**, *8*, 6964 – 6968.
[23] P. P. Pillai, S. Huda, B. Kowalczyk, B. A. Grzybowski, *J. Am. Chem. Soc.* **2013**, *135*, 6392 – 6395.
[24] M. Kanamala, W. R. Wilson, M. Yang, B. D. Palmer, Z. Wu, *Biomaterials* **2016**, *85*, 152 – 167.
[25] C. A. Monnier, D. C. Thévenaz, S. Balog, G. L. Fiore, D. Vanhecke, B. Rothen-Rutishauser, A. Petri-Fink, *AIMS Biophys.* **2015**, *2*, 245 – 258.
[26] D. P. Joshi, Y. L. Lan-Chun-Fung, J. G. Pritchard, *Anal. Chim. Acta* **1979**, *104*, 153 – 160.
[27] S. Eustis, M. A. El-Sayed, *Chem. Soc. Rev.* **2006**, *35*, 209 – 217.
[28] K. Wang, X. He, X. Yang, H. Shi, *Acc. Chem. Res.* **2013**, *46*, 1367 – 1376.

Manuscript received: May 26, 2017
Revised manuscript received: July 22, 2017
Accepted manuscript online: August 2, 2017
Version of record online: September 22, 2017

